MedChemComm

RESEARCH ARTICLE

View Article Online
View Journal

Cite this: DOI: 10.1039/c5md00401b

Novel quinoline-derived mTOR inhibitors with remarkable enzymatic and cellular activities: design, synthesis and biological evaluation

Xiao-Dong Ma, Ni Qiu, Bo Yang, Qiao-Jun He and Yong-Zhou Hu*

Received 12th September 2015,
Accepted 25th November 2015

DOI: 10.1039/c5md00401b

www.rsc.org/medchemcomm

Herein, we reported the preparation and *in vitro* development of a novel series of quinoline-based mTOR inhibitors, some of which were obtained *via* introducing a ring-opening strategy. As for enzymatic activity, more than half of these quinoline derivatives exhibited moderate to potent inhibition against mTOR. Among them, six compounds showed IC_{50} values below 50 nM. In particular, several quinolines exhibited remarkably enhanced anti-proliferative activities against all the three tested tumor cell lines in contrast to the initial lead **9**. As a representative in this series, compound **24** demonstrated IC_{50} values of 0.11, 0.17 and 0.04 μM against HCT-116, PC-3 and MCF-7 cell lines, respectively. Besides, compounds **17** and **24** were identified to be selective over class I PI3Ks. Further Western blot analysis validated the dual inhibition of mTORC1 and mTORC2 as a result of compound **24** treatment in the MCF-7 cell line, which was beneficial for conquering the S6K/IRS1/PI3K negative feedback loop. Moreover, acceptable stability was displayed by compound **17**, another representative of this series, in simulated intestinal fluid (SIF), simulated gastric fluid (SGF), as well as rat liver microsome (RLM). By virtue of the favorable biological profiles, several quinolines merit further *in vivo* investigation.

1. Introduction

The mammalian target of rapamycin (mTOR) is a critical integrator of extra- and intra-cellular signals that regulates diverse growth-related processes, exemplified by translation, metabolism, ribosome biogenesis and proliferation.[1–5] In cells, mTOR assembles into two distinct multi-protein complexes: mTORC1 and mTORC2.[6] Functionally, mTORC1 serves as the downstream regulator of Akt, while mTORC2 emerges upstream of Akt, activating it upon phosphorylation at Ser473.[7] As a drug discovery target, mTOR has inspired considerable scientific interest, due to its frequent deregulation in oncology.[8–10] Despite intensified development efforts, mTORC1 selective inhibitors, including rapamycin and its semi-synthetic analogs (rapalogues),[11,12] merely benefit patients with advanced and metastatic renal cell carcinoma (RCC).

In respect of cancer therapy, the advantages of mTOR kinase inhibitors (ATP-competitive mTOR inhibitors) over rapalogues have been widely accepted.[13] Firstly, they lead to a more complete inhibition of mTOR upon competitive interaction with the ATP-binding domain. In contrast, rapalogues only resulted in a partial suppression of mTOR in an allosteric manner. Another merit of ATP-competitive inhibitors stems from the dual inhibition of mTORC1 and mTORC2. In a myriad of cancers, the sole inhibition of mTORC1 by rapalogues releases the S6K/IRS1/PI3K negative feedback loop, consequently hyper-activating the upstream regulator Akt and neutralizing the therapeutic efficacy. Considering this, the simultaneous inhibition of mTORC2 may conquer the upregulation of Akt induced by the negative feedback loop, thereby improving clinical response and broadening the anti-tumor spectrum. In recent years, a medicinal chemistry campaign has been initiated in the exploration of mTOR kinase inhibitors to address the limitation associated with rapalogues.[14] This facilitates the clinical progression of numerous inhibitors belonging to this family, including **BEZ-235** (mTOR/PI3K dual inhibitor, **1**),[15,16] GSK-2126458 (mTOR/PI3K dual inhibitor, **2**),[17] SAR-245409 (mTOR/PI3K dual inhibitor, **3**),[18] PF-04691502 (mTOR/PI3K dual inhibitor, **4**),[19] PF-05212384 (mTOR/PI3K dual inhibitor, **5**),[20] AZD-2014 (mTOR inhibitor, **6**),[21] MLN-0128 (mTOR inhibitor, **7**)[22] and CC-223 (mTOR inhibitor, **8**)[23,24] (Fig. 1).

Our latest exploration of ATP-competitive mTOR inhibitors has culminated in a novel series of 3,4,6-trisubstituted quinoline derivatives with favorable enzymatic potency. During the further optimization to enhance their anti-proliferative activities, compound **9** in this series attracted our attention due to

Zhejiang Province Key Laboratory of Anti-Cancer Drug Research, College of Pharmaceutical Sciences, Zhejiang University, Hangzhou 310058, China.
E-mail: huyz@zju.edu.cn; Fax: +86 571 88208460; Tel: +86 571 88208460

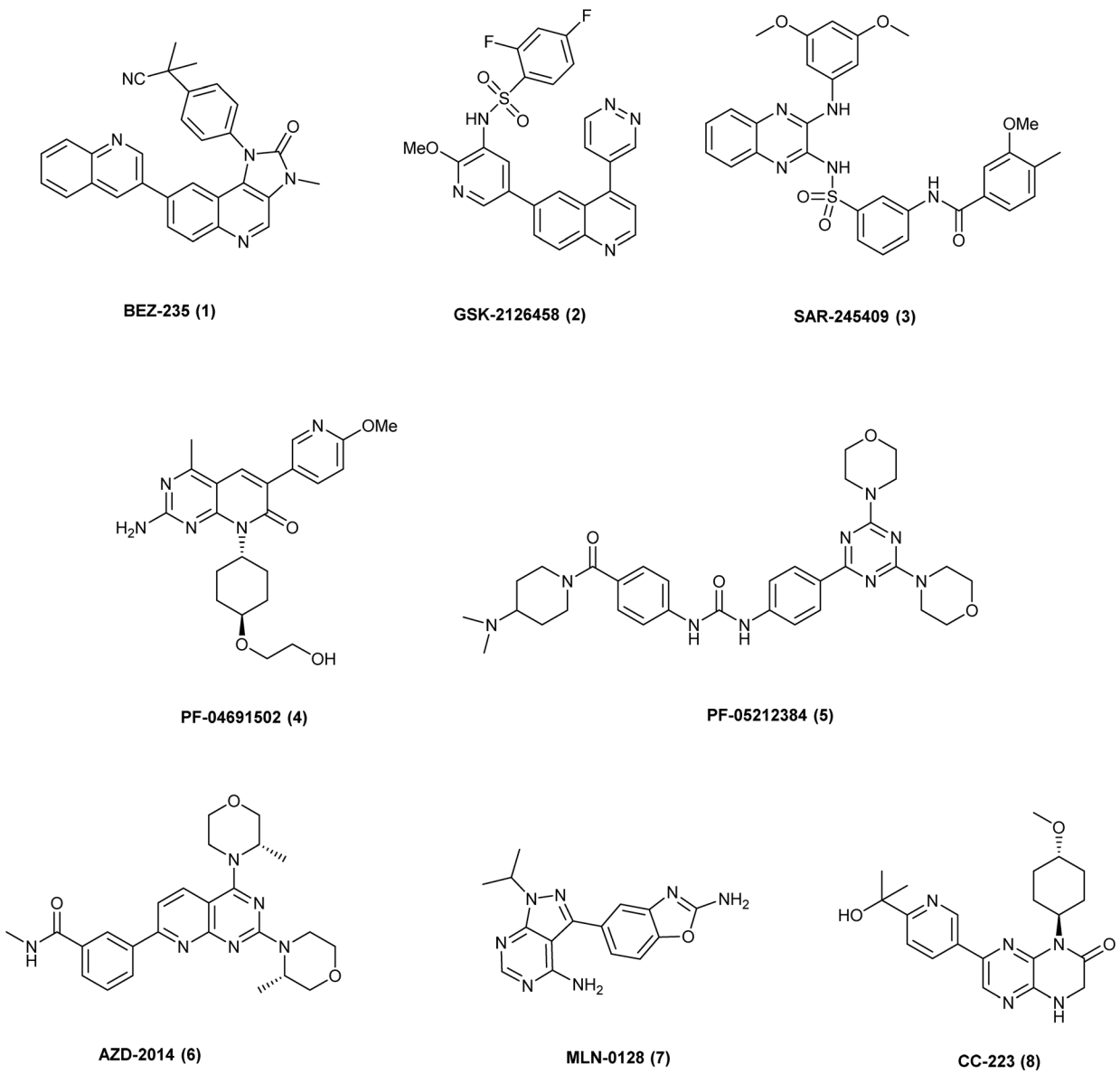

Fig. 1 Some representative mTOR kinase inhibitors under clinical trial.

its structural similarity to **BEZ-235** (**1**), an mTOR/PI3K dual inhibitor bearing the imidazo[4,5-*c*]quinolinone template. As illustrated in the biological data summarized in Fig. 2, **9** approximately maintained the potent mTOR inhibitory activity after de-constructing the five-membered imidazolone fused to the C-3 and C-4 positions of **1**. Thereby, the imidazolone was regarded to be dispensable for mTOR inhibition. With this information in hand, our optimization prioritized breaking imidazolone of the imidazo[4,5-*c*]quinolinone derivatives and investigating substituents distinct from those of **9** at the C-3 and C-4 positions of the quinoline core. Herein, we described this optimization approach that leads to the identification of several promising quinoline-derived mTOR inhibitors, which not only maintained the potent enzymatic activity, but also exhibited superior antiproliferative efficacies to **9**.

2. Results and discussion

2.1. Structural optimization of 8

The potent mTOR inhibitory activity of **9** encouraged our extensive structural alteration at the C-3 position of the quinoline core. After reversal of the C-3 amide functionality, the enzymatic activity decreased 3-fold while the cellular activity was maintained according to the biological data of **10** (Table 1). This informed us that the C-3 acetylamide moiety improved the physicochemical properties of **10** and offset the slight loss in mTOR inhibitory activity, thereby accounting for the comparable cellular activities of **9** and **10**. Considering the convenience in synthesis, we initiated our investigation on different replacements of the C-3 acetylamide moiety. Unfortunately, none of these counterparts, including the C-3 methylsulfonamide

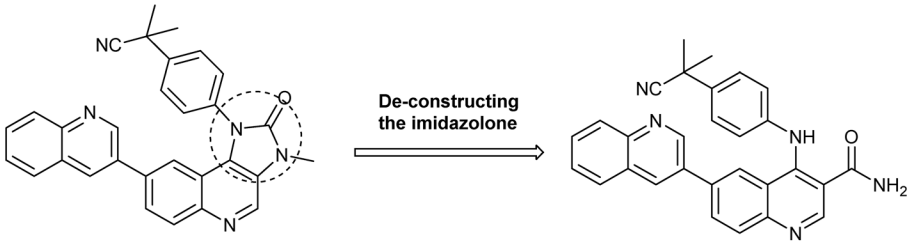

BEZ-235 (1)

mTOR (IC_{50} = 21 nM)

PI3Kα (IC_{50} = 35 nM)

HCT116 (IC_{50} = 0.20 μM)

PC-3 (IC_{50} = 0.21 μM)

MCF-7 (IC_{50} = 0.05 μM)

9

mTOR (IC_{50} = 33 nM)

PI3Kα (27% inhibition at 1 μM)

HCT116 (IC_{50} = 4.56 μM)

PC-3 (IC_{50} = 2.82 μM)

MCF-7 (IC_{50} = 0.95 μM)

Fig. 2 Structure and *in vitro* biological activities of compound **9** in contrast to those of **BEZ-235**.

Table 1 The *in vitro* biological data of compounds **10–14**

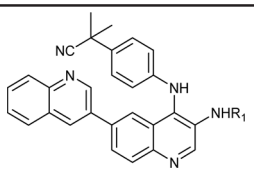

Compd	R_1	mTOR (IC_{50}, nM)	HCT-116 (IC_{50}, μM)	PC-3 (IC_{50}, μM)	MCF-7 (IC_{50}, μM)
10	CH_3CO	114	3.95	2.56	0.44
11	$MeSO_2$	[b]	>10	>10	[b]
12	CF_3CO	[a]	>10	>10	1.36
13	*t*-BuCO	[b]	>10	>10	[b]
14	$(MeSO_2)_2$	[b]	>10	>10	[b]

[a] 92% inhibition at 3000 nM. [b] Not identified.

(**11**), trifluoroacetamide (**12**), pivaloylamino (**13**) and dimethylsulfonamide (**14**), exhibited improvement in antiproliferative activities.

Bearing in mind the importance of C-6 quinoline for activity, our efforts were then directed at decorating the substituted aniline at the C-4 position. BGT-226 (**15**) was an

Table 2 The *in vitro* biological data of compounds **16–20**

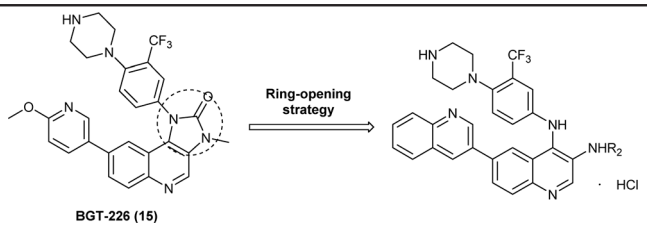

BGT-226 (15)

Compd	R_2	mTOR (IC_{50}, nM)	HCT-116 (IC_{50}, μM)	PC-3 (IC_{50}, μM)	MCF-7 (IC_{50}, μM)
16	H	46	1.61	3.44	0.47
17	CH_3CO	22	0.36	0.50	0.11
18	$MeSO_2$	340	1.45	5.42	1.11
19	CF_3CO	310	1.24	3.82	0.32
20	*t*-BuCO	17	0.64	1.05	0.30

additional dual mTOR/PI3K modulator discovered by Novartis with the same imidazo[4,5-*c*]quinolinone platform as **1**.[25] Upon introducing the ring-opening strategy, compound **16** was obtained after breaking the five-membered imidazolone and replacing the C-6 methoxypyridine with quinoline that was proven to be optimum in the former study. To our delight, this C-3 amino derivative (**16**) bearing the elongated C-4 substructure displayed an IC_{50} value of 46 nM against mTOR (Table 2). In addition, acceptable anti-proliferative efficacy was demonstrated with IC_{50} values of 1.61, 3.44 and 0.47 μM against the HCT-116, PC-3 and MCF-7 cell lines, respectively. From our point of view, compound **16** still needed diversification to modify the physicochemical profiles, especially to lower the hydrophilicity. Acetylation of the C-3 amino moiety of **16** conferred an enhanced enzymatic activity with an IC_{50} of 22 nM against mTOR. Besides, the resultant compound **17** exhibited a 4-fold, 7-fold and 4-fold increase in cellular activity against HCT-116 (IC_{50} = 0.36 μM), PC-3 (IC_{50} = 0.50 μM) and MCF-7 (IC_{50} = 0.11 μM), respectively. Subsequent introduction of methylsulfonamide or trifluoroacetamide as a C-3 substituent sharply decreased the mTOR inhibitory activity and the corresponding counterparts (**18** and **19**) only showed moderate mTOR inhibition with IC_{50} values of 340 nM and 310 nM, respectively. In response to the compromised enzymatic activity, both compounds displayed weakened anti-proliferative activities against all the tested cell lines, especially PC-3. The clear structure–activity relationships (SARs) deduced from **17–19** may give an explanation for the compromised cellular activities observed for **12** and **13**. Although compound **20** maintained the mTOR inhibitory activity of **17**, the excessive increase in hydrophobicity caused a slight loss in cellular activity after replacing the C-3 acetylamide with pivaloylamino.

Beyond that of **17**, several other substitution patterns at the phenyl ring of the C-4 aniline, including the 4-cyano, 4-trifluoromethyl, as well as 3,5-dimethyloxy replacements, were also investigated. However, all of these turned out to be detrimental to the enzymatic activity according to the biological data summarized in Table 3. Consistent with the loss in mTOR inhibitory activity, the resultant compounds **21–23** demonstrated a significant decrease in anti-proliferative efficacies against the three tumor cell lines.

As demonstrated in the molecular docking (Fig. 3), the piperazine of **17** was projected into a vast space, thereby accessible to a variety of substituents for further modulating the physicochemical properties. Simple diversification, such as acylation and sulfonylation, retained the enzymatic activity as illustrated by the comparable IC_{50} values of **24** (IC_{50} = 30 nM) and **25** (IC_{50} = 25 nM) to **17** (Table 4). However, the slight improvement in hydrophobicity did improve the anti-proliferative activities. The *N*-acetyl piperazine derivative **24** exhibited a 3-fold enhanced anti-proliferative efficacy compared to **17** against all the tested cell lines with IC_{50} values of 0.11 (HCT-116), 0.17 (PC-3) and 0.04 μM (MCF-7), respectively. The cellular activity of *N*-sulfonylated piperazine derivative **25** was also remarkable with IC_{50} values of 0.43, 0.19 and 0.06 μM against HCT-116, PC-3 and MCF-7, respectively. Similar to that observed in compound **20**, further increase in hydrophobicity *via* replacing the C-3 acetamide of **24** with pivaloylamino significantly weakened the cellular potency against MCF-7 by 20-fold, although the enzymatic activity of the resultant compound **26** varied slightly (IC_{50} = 36 nM). Up to this point, the SAR investigation described above enabled the identification of several potent mTOR inhibitors, including **17**, **24** and **25**, that displayed considerably enhanced anti-proliferative efficacies in comparison with the initial lead **9**.

2.2. Molecular docking

Before diversification at the piperazine moiety, compound **17** was docked into the catalytic cleft for probing its possible binding mode with mTOR. As illustrated in Fig. 3a, the quinoline template conferred a critical H-bond interaction with the residue Val2240 in the hinge region. Meanwhile, the carbonyl of the C-3 amide moiety served as an H-bond receptor for residue Cys2243. The quinoline replacement at the C-6 position reached into the inner hydrophobic pocket, engaging in an H-bond with residue Tyr2225. In addition to these H-bond interactions, the trifluoromethyl group packed partially into the *N*-lobe pocket (Leu2185, Pro2169, *etc.*). As described above, the piperazine was directed into a largely solvent-exposed region, thereby tolerable for further diversification. The binding mode of compound **20** was similar to that of **17** (Fig. 3b). The quinoline core, the C-3 amide and the C-6 quinoline made three contacts to residues Val2240, Cys2243 and Tyr2225 *via* H-bonds. The bulky *t*-butyl group of **20** successfully avoided the unfavorable interactions with the

Table 3 The *in vitro* biological data of compounds **21–23**

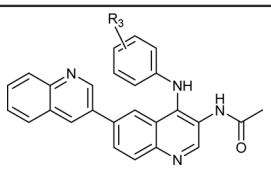

Compd	R_3	mTOR (IC_{50}, nM)	HCT-116 (IC_{50}, μM)	PC-3 (IC_{50}, μM)
21	4-CN	>3000	>10	>10
22	4-CF_3	>3000	>10	>10
23	3,5-$(OCH_3)_2$	>3000	>10	>10

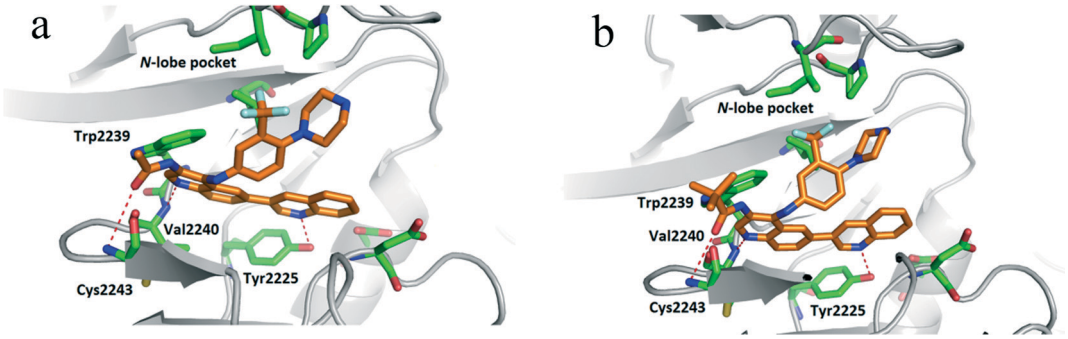

Fig. 3 Molecular docking of quinolines **17** (a) and **20** (b) into the catalytic cleft of mTOR.

Table 4 The *in vitro* biological data of compounds **24–26**

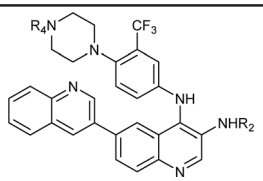

Compd	R_2	R_4	mTOR (IC_{50}, nM)	HCT-116 (IC_{50}, μM)	PC-3 (IC_{50}, μM)	MCF-7 (IC_{50}, μM)
24	CH_3CO	CH_3CO	30	0.11	0.17	0.04
25	CH_3CO	$MeSO_2$	25	0.43	0.19	0.06
26	*t*-BuCO	CH_3CO	36	>10	>10	0.79
PI-103			14			
BEZ-235			21	0.14	0.19	0.05

indole moiety of residue Trp2239, thereby accounting for its comparable mTOR inhibitory activity to that of **17**.

2.3. Chemistry

Scheme 1 displays the synthetic route for compounds **10–14** and **21–23**. 2-Aminobenzoic acid (**27**) was employed as the starting material and was firstly brominated to furnish **28**. Meanwhile, **30** was prepared from nitromethane *via* the reported method with minor modification.[26] Following condensation of **30** with **28**, the newly formed **31** was subjected to an intra-molecular cyclization to afford intermediate **32**. Afterwards, treatment of **32** with phosphorus oxychloride led to the formation of the key intermediate **33**. SNAr reaction of **33** with the corresponding substituted anilines then provided intermediates **34** or **36a–c**. Their subsequent Suzuki coupling with quinoline-3-boronic acid pinacol ester correspondingly gave **35** or **37a–c** as intermediates. Finally, they underwent catalytic hydrogenation and acylation or sulfonylation to generate target compounds **10–14** and **21–23**.

As shown in Scheme 2, the intermediate **33** was converted to **40** after a sequence of SNAr reaction, Suzuki coupling and catalytic hydrogenation. Subsequent removal of the Boc-protecting group of **40** resulted in the formation of compound **16** as the hydrochloride. Alternatively, the C-3 amino functionality of **40** was further acylated or sulfonylated to provide intermediates **41a–d**. Afterwards, their Boc-protecting groups were removed to furnish the corresponding compounds **17–20** as the hydrochlorides. Ultimately, the piperazines of compounds **17** or **20** were acetylated or sulfonylated to generate compounds **24–26**.

2.4 Selectivity over class I PI3Ks

Compounds **17** and **24** in this series were further evaluated for their inhibitory activities against PI3Kα, PI3Kβ, PI3Kγ and PI3Kδ with **PI-103** as the positive control. As summarized in Table 5, compound **17** exhibited significant inhibition to none of the four class I PI3Ks at the concentration of 1.0 μM. Besides, compound **24** also displayed acceptable specificity, which was 50-fold, >167-fold, 17-fold and 70-fold selective over PI3Kα, PI3Kβ, PI3Kγ and PI3Kδ, respectively.

2.5 Western blot assay in the MCF-7 cell line

Compound **24**, as the representative of this series, was selected for further Western blot analysis in the MCF-7 cell line, in which pS6 (Ser235) and pAkt (Ser473) served as the biomarker for the inhibition of mTORC1 and mTORC2, respectively (Fig. 4). As we anticipated, the sole inhibition of mTORC1 by rapamycin led to an obvious increase in the level of pAkt at the concentration of 0.5 μM, indicating the release of the S6K/IRS1/PI3K negative feedback loop. In contrast, compound **24** treatment induced simultaneous downregulation of pS6 (Ser235) and pAkt (Ser473) at the same concentration, implying the dual inhibition of mTORC1 and mTORC2. Moreover, compound **24** culminated in a

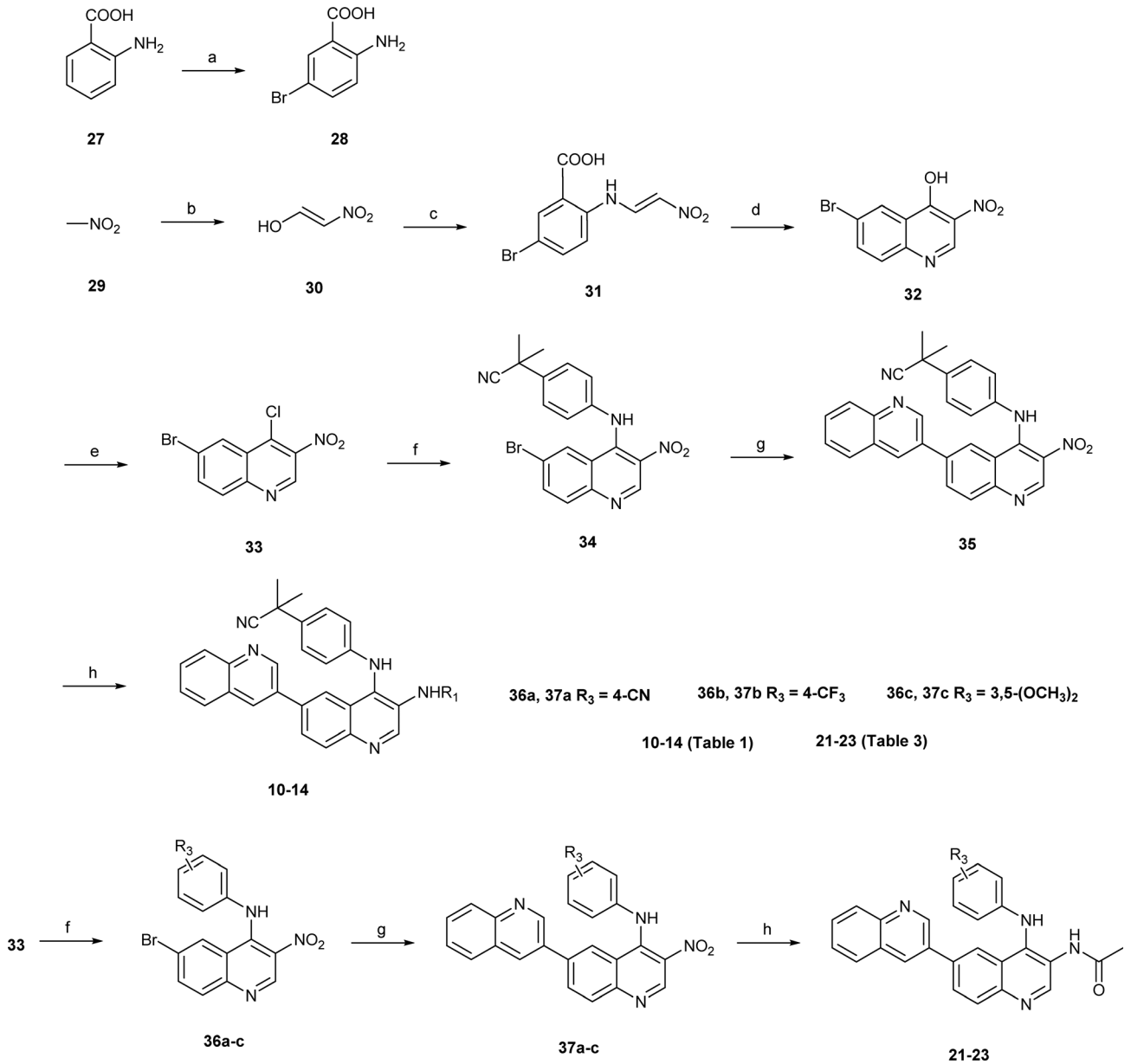

Scheme 1 Reagents and conditions: (a) NH_4Br, H_2O_2 (30%), HAc, 10 °C to rt; (b) NaOH, H_2O, 0 °C; concentrated HCl, ice; (c) **28**, EtOH, rt; (d) AcOK, Ac_2O, 120 °C; (e) DMF, $POCl_3$, reflux; (f) corresponding substituted aniline, AcONa, HAc, rt; (g) corresponding borate, K_2CO_3, $Pd(PPh_3)_4$, H_2O/1,4-dioxane, 100 °C; (h) (1) H_2, Pd/C, MeOH, rt; (2) AcCl, pyridine, THF, 0 °C (for **10**, **21**–**23**); $MeSO_2Cl$, pyridine, 40 °C (for **11**); $(CF_3CO)_2O$, pyridine, DCM, rt (for **12**); *t*-BuCOCl, pyridine, THF, 0 °C (for **13**); $MeSO_2Cl$, Et_3N, THF, rt (for **14**).

partial downregulation of pS6 (Ser235) and a complete downregulation of pAkt (Ser473) at the concentration as low as 0.1 μM. These experimental results testified the advantage of **24** over mTORC1 modulator rapamycin in conquering the S6K/IRS1/PI3K negative feedback loop.

2.6. *In vitro* stability

To guide the further *in vivo* development of these quinolines, compound **17** was subsequently chosen as their representative to investigate their stability in simulated intestinal fluid (SIF), simulated gastric fluid (SGF) and rat liver microsome (RLM). As a consequence, no obvious degradation was observed after 45 min-exposure to both SIF and SGF. In addition, it demonstrated an acceptable metabolic stability in RLM, with more than half remaining after 30 min.

3. Experimental

3.1. Chemistry

The reagents and solvents for the reactions were purchased from common commercial suppliers. If necessary, purification was carried out prior to use. Melting points were uncorrected and determined on a Büchi B-540 apparatus

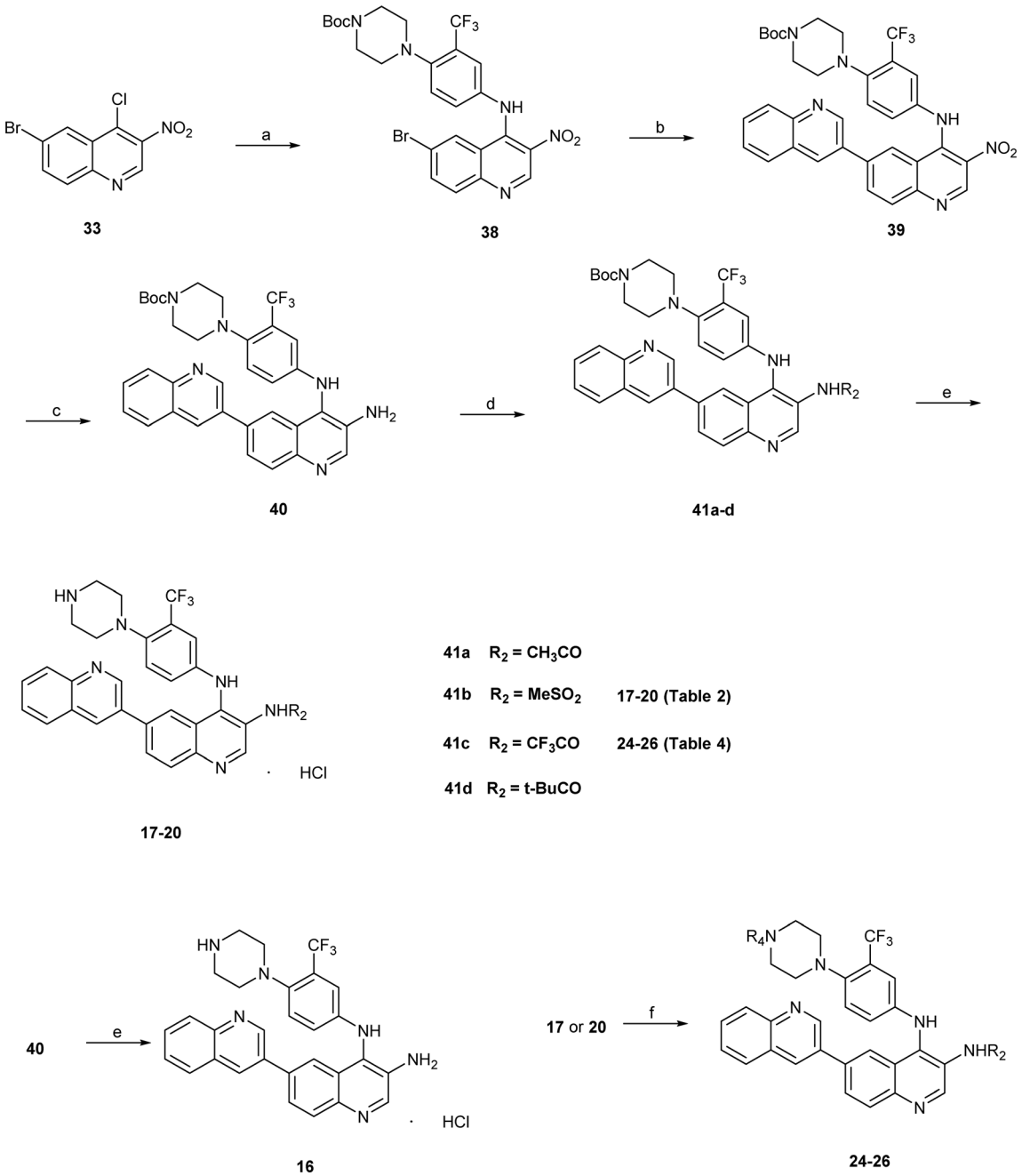

Scheme 2 Reagents and conditions: (a) corresponding substituted aniline, AcONa, HAc, rt; (b) corresponding borate, K_2CO_3, $Pd(PPh_3)_4$, H_2O/1,4-dioxane, 100 °C; (c) H_2, Pd/C, MeOH, rt; (d) AcCl, pyridine, THF, 0 °C (for **41a**); $MeSO_2Cl$, pyridine, 40 °C (for **41b**); $(CF_3CO)_2O$, pyridine, DCM, rt (for **41c**); *t*-BuCOCl, pyridine, THF, 0 °C (**41d**); (e) HCl (EtOAc solution, concentrated), 0 °C to rt; (f) Et_3N, AcCl, THF, 0 °C (for **24** and **26**); Et_3N, $MeSO_2Cl$, THF, 0 °C (for **25**).

Table 5 The inhibitory activities of compounds **17** and **24** against class I PI3Ks

Compd	PI3Kα	PI3Kβ	PI3Kγ	PI3Kδ
17	42.1%[a]	1.0%[a]	47.3%[a]	34.9%[a]
24	1500[b]	>5000[b]	502[b]	2075[b]
PI-103	12[b]	13[b]	48[b]	10[b]

[a] Inhibition rate at 1.0 μM. [b] IC_{50} value (nM).

(Büchi Labortechnik, Flawil, Switzerland). ^1H NMR and ^{13}C NMR spectra were recorded on 500 MHz (or 400 MHz) and 125 MHz (or 100 MHz) instruments, respectively, (Bruker Bioscience, Billerica, MA, USA) with tetramethylsilane (TMS) as internal standard. The ESI mass spectral data were obtained by using an Esquire-LC-00075 spectrometer (Bruker Bioscience). Flash column chromatography was performed using silica gel (200–300 mesh). HPLC was performed using an Agilent 1200 system with UV detection at 254 nm, eluting

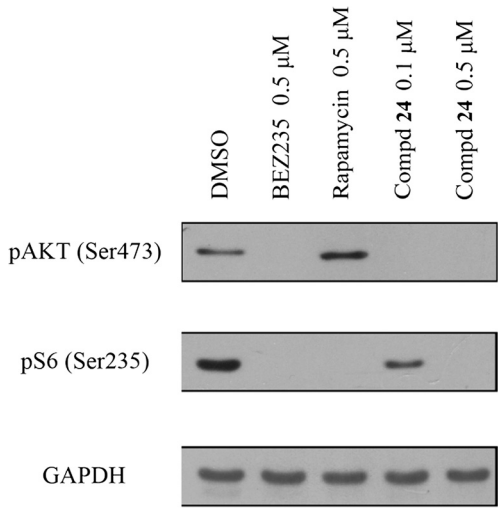

Fig. 4 Western blot analysis of the quinoline derivative **24** in the MCF-7 cell line.

with a binary solvent system A and B [A: CH_3OH; B: H_2O with 0.12% ammonium acetate (w/v)]. Analytical purity of all compounds was >95% unless stated otherwise.

3.1.1. 2-Amino-5-bromobenzoic acid (28). To a suspension of 2-aminobenzoic acid (**27**, 6.86 g, 50.0 mmol, 1.0 eq.) and ammonium bromide (5.39 g, 55.0 mmol, 1.1 eq.) in HAc (50 mL), hydrogen dioxide (6.00 mL, 30%, 55.0 mmol, 1.1 eq.) was added dropwise at 10 °C. After stirring at room temperature for 16 h, the reaction mixture was slowly poured into water and the crude product was precipitated. Following filtration, it was washed with water and compound **28** was obtained as a pale solid after recrystallization from water. Yield: 83%; mp 217–219 °C.

3.1.2. (*E*)-5-Bromo-2-(2-nitrovinylamino)benzoic acid (31). To a solution of sodium hydroxide (30.2 g, 756 mmol, 3.0 eq.) in water (70 mL), nitromethane (13 mL, 252 mmol, 1.0 eq.) was dropwise at 0 °C. The reaction mixture was stirred at the same temperature for 1 h and at room temperature for another hour. Then, it was slowly poured to a mixture of ice (60.0 g) and concentrated HCl (90.0 mL). The resultant solution was immediately combined with a solution of **28** (6.03 g, 27.9 mmol, 0.11 eq.) in EtOH (450 mL) and the mixture was allowed to be stirred at room temperature for 18 h. Following filtration, the solid product was washed repeatedly with water. The cake was sliced into flakes and dried *in vacuo* at 35 °C to provide the title compound as a yellow solid, which was used directly for the next step. Yield: 78%.

3.1.3. 6-Bromo-3-nitroquinolin-4-ol (32). A mixture of **31** (5.74 g, 20.0 mmol, 1.0 eq.), potassium acetate (2.35 g, 24.0 mmol, 1.2 eq.) and acetic anhydride (30 mL) was stirred at 120 °C for 2 h. After cooling, the precipitate was filtered and washed repeatedly with acetic acid, and then with water. Afterwards, it was dried to give the title product. Yield: 38%; ESI-MS: m/z = 267 $[M + H]^-$.

3.1.4. 6-Bromo-4-chloro-3-nitroquinoline (33). To a suspension of **32** (1.61 g, 6.00 mmol) in phosphorus oxychloride (10 mL), a catalytic amount of DMF was added, and the mixture was stirred under reflux for 4 h. Then, it was cooled and slowly poured onto ice. Afterwards, the precipitate was filtered, washed with water and dissolved in dichloromethane (DCM). The solution was subsequently washed with a saturated $NaHCO_3$ solution, brine, dried with anhydrous Na_2SO_4 and concentrated *in vacuo*. The residue was purified *via* flash column chromatography using ethyl acetate (EA)/petroleum ether (PE) (1 : 10) as the eluent to afford **33** as a white solid. Yield: 92%; ^{1}H NMR (500 MHz, $CDCl_3$): 9.21 (s, 1H, Ar–H), 8.47 (s, 1H, Ar–H), 8.02 (d, 9.0 Hz, 1H, Ar–H), 7.95 (d, 9.0 Hz, 1H, Ar–H); ESI-MS: m/z = 287 $[M + H]^+$.

3.1.5. General procedure for the preparation of intermediates 34, 36a–c and 38 (A). To a solution of **33** (1.0 eq.) in acetic acid (2 mL per 1 mmol of substrate), AcONa (1.4 eq.) and 2-(4-aminophenyl)-2-methylpropanenitrile (1.0 eq.) were added at room temperature. The resultant mixture was stirred for 0.5 h at the same temperature and quenched with water. After the crude product was totally precipitated, it was filtered, washed with water and dissolved in DCM. The resultant solution was subsequently washed with a saturated $NaHCO_3$ solution, brine, and dried over anhydrous Na_2SO_4. Following removal of DCM *in vacuo*, the residue was purified *via* flash column chromatography using EA/PE (1 : 6) as the eluent to afford 2-(4-((6-bromo-3-nitroquinolin-4-yl)amino)-phenyl)-2-methylpropanenitrile (**34**) as a light yellow solid. The intermediates **36a–c** and **38** were prepared according to the procedure for **34**, only with 2-(4-aminophenyl)-2-methylpropanenitrile replaced by the corresponding substituted aniline, including 4-aminobenzonitrile (for **36a**), 4-(trifluoromethyl)aniline (for **36b**), 3,5-dimethoxyaniline (for **36c**) and *tert*-butyl 4-(4-amino-3-(trifluoromethyl)phenyl)-piperazine-1-carboxylate (for **38**).

3.1.5.1. 2-(4-((6-Bromo-3-nitroquinolin-4-yl)amino)phenyl)-2-methylpropanenitrile (34). Light yellow solid; yield: 86%; ^{1}H NMR (400 MHz, DMSO-d_6): 10.12 (s, 1H, NH), 9.09 (s, 1H, Ar–H), 8.71 (s, 1H, Ar–H), 8.02 (d, 8.8 Hz, 1H, Ar–H), 7.94 (d, 8.8 Hz, 1H, Ar–H), 7.47 (d, 8.4 Hz, 2H, Ar–H), 7.14 (d, 8.4 Hz, 2H, Ar–H), 1.68 (s, 6H, CH_3 × 2); ESI-MS: m/z = 411 $[M + H]^+$.

3.1.5.2. 4-((6-Bromo-3-nitroquinolin-4-yl)amino)benzonitrile (36a). Light yellow crystal; yield: 83%; ^{1}H NMR (400 MHz, DMSO-d_6): 10.09 (s, 1H, NH), 9.06 (s, 1H, Ar–H), 8.79 (s, 1H, Ar–H), 8.02 (d, 8.4 Hz, 1H, Ar–H), 7.95 (d, 8.4 Hz, 1H, Ar–H), 7.30 (d, 8.4 Hz, 2H, Ar–H), 7.11 (d, 8.4 Hz, 2H, Ar–H); ESI-MS: m/z = 369 $[M + H]^+$.

3.1.5.3. 6-Bromo-3-nitro-N-(4-(trifluoromethyl)phenyl)-quinolin-4-amine (36b). Light yellow solid; yield: 91%; ^{1}H NMR (500 MHz, $CDCl_3$): 10.31 (s, 1H, NH), 9.52 (s, 1H, Ar–H), 7.98 (d, 9.0 Hz, 1H, Ar–H), 7.85 (dd, 2.0 Hz, 9.0 Hz, 1H, Ar–H), 7.78 (d, 2.0 Hz, 1H, Ar–H), 7.68 (d, 8.0 Hz, 2H, Ar–H), 7.22 (d, 8.0 Hz, 2H, Ar–H); ESI-MS: m/z = 412 $[M + H]^+$.

3.1.5.4. 6-Bromo-N-(3,5-dimethoxyphenyl)-3-nitroquinolin-4-amine (36c). Light yellow solid; yield: 86%; ^{1}H NMR (400 MHz, DMSO-d_6): 10.00 (s, 1H, NH), 9.05 (s, 1H, Ar–H), 8.78 (s, 1H, Ar–H), 8.02 (d, 8.8 Hz, 1H, Ar–H), 7.94 (d, 8.8 Hz, 1H,

Ar–H), 6.26 (s, 3H, Ar–H), 3.69 (s, 6H, OCH_3 × 2); ESI-MS: *m*/*z* = 404 $[M + H]^+$.

3.1.5.5 tert-Butyl 4-(4-((6-bromo-3-nitroquinolin-4-yl)amino)-2-(trifluoromethyl)phenyl)piperazine-1-carboxylate (38). Light yellow solid; yield: 88%; ^{1}H NMR (400 MHz, DMSO-d_6): 10.16 (s, 1H, NH), 9.09 (s, 1H, Ar–H), 8.71 (s, 1H, Ar–H), 8.03 (d, 9.2 Hz, 1H, Ar–H), 7.95 (d, 9.2 Hz, 1H, Ar–H), 7.52 (d, 8.4 Hz, 1H, Ar–H), 7.41 (s, 1H, Ar–H), 7.31 (d, 8.4 Hz, 1H, Ar–H), 3.46–3.40 (m, 4H, piperazine–CH_2 × 2), 2.82–2.75 (m, 4H, piperazine–CH_2 × 2), 1.43 (s, 9H, CH_3 × 3); ESI-MS: *m*/*z* = 596 $[M + H]^+$.

3.1.6. General procedure for the preparation of intermediates 35, 37a–c and 39 (B). To a solution of **34** (1.0 eq.) in H_2O/1,4-dioxane (1 : 3, v/v, 12 mL per 1 mmol of substrate), anhydrous potassium carbonate (1.1 eq.), quinoline-3-boronic acid pinacol ester (1.1 eq.) and $Pd(Ph_3P)_4$ (0.08 eq.) were added. The resultant suspension was stirred at 100 °C for 8 h under N_2 atmosphere. After this time, the reaction mixture was removed from the oil bath, cooled and concentrated *in vacuo*. The residue was treated with EtOAc, and following filtration, the filtrate was washed with water and brine. Afterwards, the organic layer was dried over anhydrous Na_2SO_4 and concentrated *in vacuo*. The residue was subjected to flash column chromatography using EA/DCM (1 : 3–1 : 1) as the eluent, which afforded **35** as a yellow solid. The intermediates **37a–c** and **39** were prepared according to the procedure for **35**, only with **34** replaced by **36a–c** or **38** as the substrate.

3.1.6.1. 2-Methyl-2-(4-((3′-nitro-[3,6′-biquinolin]-4′-yl)amino)-phenyl)propanenitrile (35). Yellow solid; yield: 82%; 1H NMR (500 MHz, $CDCl_3$): 10.66 (s, 1H, NH), 9.54 (s, 1H, Ar–H), 8.61 (d, 1.5 Hz, 1H, Ar–H), 8.19 (d, 9.0 Hz, 1H, Ar–H), 8.11 (d, 8.5 Hz, 1H, Ar–H), 8.08 (dd, 2.0 Hz, 8.5 Hz, 1H, Ar–H), 7.99 (d, 1.0 Hz, 1H, Ar–H), 7.97 (d, 2.0 Hz, 1H, Ar–H), 7.82 (d, 8.0 Hz, 1H, Ar–H), 7.76–7.72 (m, 1H, Ar–H), 7.62–7.59 (m, 3H, Ar–H), 7.30 (d, 8.5 Hz, 2H, Ar–H), 1.78 (s, 6H, CH_3 × 2); ESI-MS: *m*/*z* = 460 $[M + H]^+$.

3.1.6.2. 4-((3′-Nitro-[3,6′-biquinolin]-4′-yl)amino)benzonitrile (37a). Yellow solid; yield: 77%; ESI-MS: *m*/*z* = 418 $[M + H]^+$.

3.1.6.3. 3′-Nitro-N-(4-(trifluoromethyl)phenyl)-[3,6′-biquinolin]-4′-amine (37b). Yellow solid; yield: 68%; ESI-MS: *m*/*z* = 461 $[M + H]^+$.

3.1.6.4. N-(3,5-Dimethoxyphenyl)-3′-nitro-[3,6′-biquinolin]-4′-amine (37c). Yellow solid; yield: 79%; ^{1}H NMR (500 MHz, $CDCl_3$): 10.65 (s, 1H, NH), 9.51 (s, 1H, Ar–H), 8.86 (d, 2.0 Hz, 1H, Ar–H), 8.17–8.15 (m, 3H, Ar–H), 8.08 (dd, 2.0 Hz, 8.5 Hz, 1H, Ar–H), 7.94 (s, 1H, Ar–H), 7.80 (d, 8.0 Hz, 1H, Ar–H), 7.78–7.75 (m, 1H, Ar–H), 7.64–7.61 (m, 1H, Ar–H), 6.58 (t, 2.0 Hz, 1H, Ar–H), 6.42 (d, 2.0 Hz, 2H, Ar–H), 3.77 (s, 6H, OCH_3 × 2); ESI-MS: *m*/*z* = 453 $[M + H]^+$.

3.1.6.5. tert-Butyl 4-(4-((3′-nitro-[3,6′-biquinolin]-4′-yl)amino)-2-(trifluoromethyl)phenyl)piperazine-1-carboxylate (39). Yellow solid; yield: 70%; ^{1}H NMR (500 MHz, $CDCl_3$): 10.28 (s, 1H, NH), 9.28 (d, 2.5 Hz, 1H, Ar–H), 9.12 (s, 1H, Ar–H), 8.82 (d, 2.0 Hz, 1H, Ar–H), 8.74 (d, 2.0 Hz, 1H, Ar–H), 8.42 (d, 8.5 Hz, 1H, Ar–H), 8.16 (d, 8.5 Hz, 1H, Ar–H), 8.08–8.05 (m, 2H, Ar–H), 7.81–7.78 (m, 1H, Ar–H), 7.69–7.66 (m, 1H, Ar–H), 7.55 (d, 9.0 Hz, 1H, Ar–H), 7.49 (s, 1H, Ar–H), 7.37 (d, 9.0 Hz, 1H, Ar–H), 3.44–3.37 (m, 4H, piperazine–CH_2 × 2), 2.77 (t, 4.5 Hz, 4H, piperazine–CH_2 × 2), 1.41 (s, 9H, CH_3 × 3); ESI-MS: *m*/*z* = 645 $[M + H]^+$.

3.1.7. Synthetic procedures for compounds 10–14, 21–23 and intermediates 41a–d. To a suspension of the intermediate **35** in methanol, 10% Pd/C (10% of the weight of the substrate) was added. The resultant mixture was stirred under H_2 (balloon) overnight at room temperature. After this time, Pd/C was filtered and the filtrate was concentrated *in vacuo* to provide the C-3 amino derivative as a colorless oil, which was used for the next step without purification.

Subsequently, the newly formed C-3 amino derivative (1.0 eq.) and pyridine (1.1 eq.) were dissolved in anhydrous THF (5 mL per 1 mmol of substrate). Afterwards, a solution of acetyl chloride (1.1 eq.) in anhydrous tetrahydrofuran (THF, 5 mL per 1 mmol of substrate) was added dropwise to the mixture at 0 °C. The resultant mixture was stirred at the same temperature for 30 min and then concentrated *in vacuo*. The residue was dissolved in DCM, and the solution was washed with a saturated $NaHCO_3$ solution and brine. The organic layer was subsequently dried over anhydrous Na_2SO_4 and concentrated *in vacuo*. Afterwards, the residue was subjected to flash column chromatography with EA/MeOH (50 : 1) as the eluent to give the target compound **10** as a light yellow solid.

The solution of the newly formed C-3 amino derivative (1.0 eq.) and methylsulfonyl chloride (1.0 eq.) in anhydrous pyridine (4 mL per 1 mmol of substrate) was warmed at 40 °C under N_2 atmosphere. After 8 h, the mixture was directly subjected to flash column chromatography with EA/MeOH (50 : 1) as the eluent to give the target compound **11** as a light yellow solid.

The solution of the newly formed C-3 amino derivative (1.0 eq.), pyridine (1.2 eq.) and trifluoroacetic anhydride (1.2 eq.) in anhydrous DCM (10 mL per 1 mmol of substrate) was stirred at room temperature under N_2 atmosphere for 2 h. Afterwards, the reaction mixture was washed with a saturated $NaHCO_3$ solution and brine. The organic layer was subsequently dried over anhydrous Na_2SO_4 and concentrated *in vacuo*. Afterwards, the residue was subjected to flash column chromatography with EA as the eluent to give the target compound **12**.

The newly formed C-3 amino derivative (1.0 eq.) and pyridine (1.1 eq.) were dissolved in anhydrous THF (5 mL per 1 mmol of substrate). Afterwards, a solution of pivaloyl chloride (1.1 eq.) in anhydrous THF (5 mL per 1 mmol of substrate) was added dropwise to the mixture at 0 °C. The resultant mixture was stirred at the same temperature for 30 min and then concentrated *in vacuo*. The residue was dissolved in DCM, and the solution was washed with a saturated $NaHCO_3$ solution and brine. The organic layer was subsequently dried over anhydrous Na_2SO_4 and concentrated *in vacuo*. Afterwards, the residue was subjected to flash column chromatography with EA/MeOH (50 : 1) as the eluent to give the target compound **13** as a light yellow solid.

To a solution of the newly formed C-3 amino derivative (1.0 eq.) and Et_3N (TEA, 4.0 eq.) in anhydrous THF (10 mL per 1 mmol of substrate), methanesulfonyl chloride (4.0 eq.) was added at room temperature. The resultant mixture was stirred at the same temperature for 1 h and then concentrated *in vacuo*. The residue was dissolved in DCM, and the solution was washed with a saturated $NaHCO_3$ solution and brine. The organic layer was subsequently dried over anhydrous Na_2SO_4 and concentrated *in vacuo*. Afterwards, flash column chromatography of the residue with EA/PE (1 : 2–3 : 4) as the eluent gave the target compound **14**.

Compounds **21–23** and the intermediate **41a** were prepared according to the procedure for **10**, only with **35** replaced by **37a–c** or **39** as the starting material. The intermediate **41b** was prepared according to the procedure for **11**, only with **35** replaced by **39** as the starting material. The intermediate **41c** was prepared according to the procedure for **12**, only with **35** replaced by **39** as the starting material. The intermediate **41d** was prepared according to the procedure for **13**, only with **35** replaced by **39** as the starting material.

*3.1.7.1. N-(4′-((4-(2-Cyanopropan-2-yl)phenyl)amino)-[3,6′-biquinolin]-3′-yl)acetamide (**10**).* Light yellow solid; yield: 63% (for two steps); ^{1}H NMR (500 MHz, $CDCl_3$): 9.03 (s, 1H, Ar–H), 9.01 (s, 1H, Ar–H), 8.23–8.18 (m, 2H, Ar–H), 8.14 (s, 1H, Ar–H), 8.09 (d, 8.5 Hz, 1H, Ar–H), 8.00 (d, 8.0 Hz, 1H, Ar–H), 7.82 (d, 8.0 Hz, 1H, Ar–H), 7.72 (t, 7.5 Hz, 1H, Ar–H), 7.57 (t, 7.5 Hz, 1H, Ar–H), 7.35 (d, 7.5 Hz, 2H, Ar–H), 6.83 (d, 7.5 Hz, 2H, Ar–H), 2.19 (s, 3H, acetyl), 1.70 (s, 6H, CH_3 × 2); ^{13}C NMR (125 MHz, DMSO-d_6): δ 168.90, 151.29, 150.05, 147.34, 146.49, 142.58, 138.31, 134.55, 133.97, 133.69, 132.79, 130.63, 130.21, 129.19, 128.86, 128.14, 128.05, 127.65, 125.62, 125.40, 124.09, 122.41, 122.18, 118.41, 36.49, 28.94, 23.11; ESI-MS: m/z = 472 $[M + H]^+$; mp 141–142 °C; HPLC: t_R = 9.42 min, flow rate 1.0 mL min^{-1}, COSMOSIL 5C18-MS-II column (4.6 ID × 250 mm), rt, eluent A – 70%, eluent B – 30%.

*3.1.7.2. N-(4′-((4-(2-Cyanopropan-2-yl)phenyl)amino)-[3,6′-biquinolin]-3′-yl)methanesulfonamide (**11**).* Light yellow solid; yield: 46% (for two steps); ^{1}H NMR (500 MHz, DMSO-d_6): 9.25 (s, 1H, NH), 8.96 (d, 2.0 Hz, 1H, Ar–H), 8.76 (s, 1H, Ar–H), 8.64 (s, 1H, NH), 8.53 (d, 2.0 Hz, 1H, Ar–H), 8.20 (dd, 2.0 Hz, 8.5 Hz, 1H, Ar–H), 8.18 (d, 2.0 Hz, 1H, Ar–H), 8.13 (d, 8.5 Hz, 1H, Ar–H), 8.02 (d, 8.5 Hz, 1H, Ar–H), 7.98 (d, 8.5 Hz, 1H, Ar–H), 7.77–7.74 (m, 1H, Ar–H), 7.66–7.62 (m, 1H, Ar–H), 7.40 (d, 8.5 Hz, 2H, Ar–H), 6.92 (d, 8.5 Hz, 2H, Ar–H), 2.93 (s, 3H, methylsulfonyl), 1.67 (s, 6H, CH_3 × 2); ESI-MS: m/z = 508 $[M + H]^+$; mp 132–134 °C.

*3.1.7.3. N-(4′-((4-(2-Cyanopropan-2-yl)phenyl)amino)-[3,6′-biquinolin]-3′-yl)-2,2,2-trifluoroacetamide (**12**).* Light yellow solid; yield: 54% (for two steps); ^{1}H NMR (400 MHz, DMSO-d_6): 11.03 (brs, 1H, NH), 10.62 (brs, 1H, NH), 9.46 (s, 1H, Ar–H), 9.10 (s, 1H, Ar–H), 8.90 (s, 1H, Ar–H), 8.87 (s, 1H, Ar–H), 8.58 (d, 8.8 Hz, 1H, Ar–H), 8.22 (d, 8.8 Hz, 1H, Ar–H), 8.12 (d, 8.8 Hz, 2H, Ar–H), 7.87–7.81 (m, 1H, Ar–H), 7.74–7.70 (m, 1H, Ar–H), 7.54 (d, 8.0 Hz, 2H, Ar–H), 7.22 (d, 8.0 Hz, 2H, Ar–H), 1.70 (s, 6H, CH_3 × 2); ^{13}C NMR (100 MHz, DMSO-d_6): δ 158.20 ($J_{C–F}$ 34.00 Hz), 149.33, 147.81, 146.87, 145.65, 145.33, 138.88, 138.18, 135.87, 134.04, 131.88, 131.14, 130.31, 128.57, 128.53, 127.48, 125.80, 125.32, 124.44, 123.61, 123.41, 122.00, 120.64, 116.00 ($J_{C–F}$ 230.00 Hz), 112.76, 36.49, 28.33; ESI-MS: m/z = 526 $[M + H]^+$; mp 205–207 °C; HPLC: t_R = 13.90 min, flow rate 1.0 mL min^{-1}, COSMOSIL 5C18-MS-II column (4.6 ID × 250 mm), rt, eluent A – 70%, eluent B – 30%.

*3.1.7.4. N-(4′-((4-(2-Cyanopropan-2-yl)phenyl)amino)-[3,6′-biquinolin]-3′-yl)pivalamide (**13**).* Light yellow solid; yield: 71% (for two steps); ^{1}H NMR (500 MHz, DMSO-d_6): 9.43 (d, 2.0 Hz, 1H, Ar–H), 8.89 (s, 1H, NH), 8.79 (d, 2.0 Hz, 1H, Ar–H), 8.74 (d, 2.0 Hz, 1H, Ar–H), 8.66 (s, 1H, NH), 8.62 (s, 1H, Ar–H), 8.24 (dd, 2.0 Hz, 8.5 Hz, 1H, Ar–H), 8.12 (d, 8.5 Hz, 1H, Ar–H), 8.10–8.05 (m, 2H, Ar–H), 7.80–7.76 (m, 1H, Ar–H), 7.67–7.63 (m, 1H, Ar–H), 7.32 (d, 8.5 Hz, 2H, Ar–H), 6.83 (d, 8.5 Hz, 2H, Ar–H), 1.62 (s, 6H, CH_3 × 2), 0.85 (s, 9H, CH_3 × 3); ESI-MS: m/z = 514 $[M + H]^+$; mp 113–115 °C; HPLC: t_R = 9.01 min, flow rate 1.0 mL min^{-1}, COSMOSIL 5C18-MS-II column (4.6 ID × 250 mm), rt, eluent A – 70%, eluent B – 30%.

*3.1.7.5. N-(4′-((4-(2-Cyanopropan-2-yl)phenyl)amino)-[3,6′-biquinolin]-3′-yl)-N-(methylsulfonyl)methanesulfonamide (**14**).* Light yellow solid; yield: 39% (for two steps); ^{1}H NMR (500 MHz, DMSO-d_6): 8.81 (s, 1H, NH), 8.77 (s, 1H, Ar–H), 8.67 (d, 2.0 Hz, 1H, Ar–H), 8.42 (d, 2.0 Hz, 1H, Ar–H), 8.26 (dd, 2.0 Hz, 8.5 Hz, 1H, Ar–H), 8.14 (d, 8.5 Hz, 1H, Ar–H), 8.01 (d, 8.5 Hz, 1H, Ar–H), 7.99 (d, 2.0 Hz, 1H, Ar–H), 7.96 (d, 8.5 Hz, 1H, Ar–H), 7.78–7.75 (m, 1H, Ar–H), 7.65–7.61 (m, 1H, Ar–H), 7.50 (d, 8.5 Hz, 2H, Ar–H), 7.07 (d, 8.5 Hz, 2H, Ar–H), 3.55 (s, 6H, methylsulfonyl × 2), 1.69 (s, 6H, CH_3 × 2) ; ESI-MS: m/z = 586 $[M + H]^+$; mp 172–175 °C; HPLC: t_R = 7.21 min, flow rate 1.0 mL min^{-1}, COSMOSIL 5C18-MS-II column (4.6 ID × 250 mm), rt, eluent A – 70%, eluent B – 30%.

*3.1.7.6. N-(4′-((4-Cyanophenyl)amino)-[3,6′-biquinolin]-3′-yl)-acetamide (**21**).* Light yellow solid; yield: 65% (for two steps); ^{1}H NMR (500 MHz, DMSO-d_6): 9.67 (s, 1H, NH), 9.30 (d, 2.0 Hz, 1H, Ar–H), 9.25 (s, 1H, NH), 8.93 (s, 1H, Ar–H), 8.73 (d, 2.0 Hz, 1H, Ar–H), 8.46 (d, 2.0 Hz, 1H, Ar–H), 8.24 (dd, 2.0 Hz, 9.0 Hz, 1H, Ar–H), 8.16 (d, 9.0 Hz, 1H, Ar–H), 8.06 (d, 8.5 Hz, 2H, Ar–H), 7.80–7.77 (m, 1H, Ar–H), 7.68–7.64 (m, 1H, Ar–H), 7.60 (d, 8.5 Hz, 2H, Ar–H), 6.78 (d, 9.0 Hz, 2H, Ar–H), 1.83 (s, 3H, acetyl); ESI-MS: m/z = 430 $[M + H]^+$; mp 165–167 °C.

*3.1.7.7. N-(4′-((4-(Trifluoromethyl)phenyl)amino)-[3,6′-biquinolin]-3′-yl)acetamide (**22**).* Light yellow solid; yield: 52% (for two steps); ^{1}H NMR (500 MHz, $CDCl_3$): 8.90 (s, 1H, Ar–H), 8.82 (s, 1H, Ar–H), 8.30 (d, 1.5 Hz, 1H, Ar–H), 8.16 (d, 8.5 Hz, 1H, Ar–H), 8.10 (d, 8.0 Hz, 1H, Ar–H), 8.00 (s, 1H, Ar–H), 7.96 (dd, 1.5 Hz, 8.0 Hz, 1H, Ar–H), 7.87 (d, 8.0 Hz, 1H, Ar–H), 7.77–7.73 (m, 1H, Ar–H), 7.62–7.57 (m, 1H, Ar–H), 7.22 (d, 8.0 Hz, 2H, Ar–H), 6.65 (d, 8.0 Hz, 2H, Ar–H), 2.20 (s, 3H, acetyl); ESI-MS: m/z = 473 $[M + H]^+$; mp 187–188 °C; HPLC: t_R = 12.78 min, flow rate 1.0 mL min^{-1}, COSMOSIL 5C18-MS-II column (4.6 ID × 250 mm), rt, eluent A – 85%, eluent B – 15%.

*3.1.7.8. N-(4′-((3,5-Dimethoxyphenyl)amino)-[3,6′-biquinolin]-3′-yl)acetamide (**23**).* Light yellow solid; yield: 74% (for two steps); ^{1}H NMR (500 MHz, DMSO-d_6): 9.43 (s, 1H, NH), 9.32

(d, 2.0 Hz, 1H, Ar–H), 8.80 (s, 1H, NH), 8.71 (d, 2.0 Hz, 1H, Ar–H), 8.64 (s, 1H, Ar–H), 8.54 (d, 2.0 Hz, 1H, Ar–H), 8.20 (dd, 2.0 Hz, 8.5 Hz, 1H, Ar–H), 8.11 (d, 8.5 Hz, 1H, Ar–H), 8.07 (s, 1H, Ar–H), 8.05 (s, 1H, Ar–H), 7.80–7.76 (m, 1H, Ar–H), 7.68–7.64 (m, 1H, Ar–H), 6.06 (t, 2.0 Hz, 1H, Ar–H), 5.96 (d, 2.0 Hz, 2H, Ar–H), 3.63 (s, 6H, OCH_3 × 2), 1.83 (s, 3H, acetyl); ESI-MS: m/z = 465 $[M + H]^+$; mp 170–172 °C.

*3.1.7.9. tert-Butyl 4-(4-((3′-acetamido-[3,6′-biquinolin]-4′-yl)amino)-2-(trifluoromethyl)phenyl)piperazine-1-carboxylate (**41a**).* Light yellow solid; yield: 66% (for two steps); ^{1}H NMR (500 MHz, DMSO-d_6): 9.37 (s, 1H, NH), 9.35 (d, 2.5 Hz, 1H, Ar–H), 9.01 (s, 1H, NH), 8.77–8.75 (m, 2H, Ar–H), 8.61 (d, 2.0 Hz, 1H, Ar–H), 8.22 (dd, 2.0 Hz, 9.0 Hz, 1H, Ar–H), 8.11 (d, 9.0 Hz, 1H, Ar–H), 8.08–8.05 (m, 2H, Ar–H), 7.80–7.76 (m, 1H, Ar–H), 7.68–7.64 (m, 1H, Ar–H), 7.43 (d, 8.5 Hz, 1H, Ar–H), 7.09 (d, 2.5 Hz, 1H, Ar–H), 6.91 (dd, 2.5 Hz, 1H, 8.5 Hz, Ar–H), 3.45–3.37 (m, 4H, piperazine–CH_2 × 2), 2.73 (t, 5.0 Hz, 4H, piperazine–CH_2 × 2), 1.68 (s, 3H, acetyl), 1.40 (s, 9H, CH_3 × 3); ESI-MS: m/z = 657 $[M + H]^+$.

*3.1.7.10. tert-Butyl 4-(4-((3′-(methylsulfonamido)-[3,6′-biquinolin]-4′-yl)amino)-2-(trifluoromethyl)phenyl)piperazine-1-carboxylate (**41b**).* Light yellow solid; yield: 41% (for two steps); ^{1}H NMR (500 MHz, DMSO-d_6): 9.28 (s, 1H, NH), 9.08 (d, 2.5 Hz, 1H, Ar–H), 8.82 (s, 1H, NH), 8.78 (s, 1H, Ar–H), 8.60 (d, 1.5 Hz, 1H, Ar–H), 8.25 (d, 1.5 Hz, 1H, Ar–H), 8.23 (dd, 1.5 Hz, 8.5 Hz, 1H, Ar–H), 8.14 (d, 8.5 Hz, 1H, Ar–H), 8.04 (d, 8.5 Hz, 1H, Ar–H), 8.00 (d, 8.0 Hz, 1H, Ar–H), 7.81–7.75 (m, 1H, Ar–H), 7.68–7.62 (m, 1H, Ar–H), 7.45 (d, 8.5 Hz, 1H, Ar–H), 7.20 (d, 2.5 Hz, 1H, Ar–H), 7.00 (dd, 2.5 Hz, 8.5 Hz, 1H, Ar–H), 3.46–3.33 (m, 4H, piperazine–CH_2 × 2), 2.96 (s, 3H, methylsulfonyl), 2.74 (t, 5.0 Hz, 4H, piperazine–CH_2 × 2), 1.40 (s, 9H, CH_3 × 3); ESI-MS: m/z = 693 $[M + H]^+$.

*3.1.7.11. tert-Butyl 4-(4-((3′-(2,2,2-trifluoroacetamido)-[3,6′-biquinolin]-4′-yl)amino)-2-(trifluoromethyl)phenyl)piperazine-1-carboxylate (**41c**).* Light yellow solid; yield: 69% (for two steps); ESI-MS: m/z = 711 $[M + H]^+$.

*3.1.7.12. tert-Butyl 4-(4-((3′-pivalamido-[3,6′-biquinolin]-4′-yl)amino)-2-(trifluoromethyl)phenyl)piperazine-1-carboxylate (**41d**).* Light yellow solid; yield: 77% (for two steps); ^{1}H NMR (500 MHz, DMSO-d_6): 9.44 (d, 2.5 Hz, 1H, Ar–H), 9.03 (s, 1H, NH), 8.83–8.80 (m, 2H, Ar–H, NH), 8.73 (d, 2.0 Hz, 1H, Ar–H), 8.64 (s, 1H, Ar–H), 8.25 (dd, 2.0 Hz, 8.5 Hz, 1H, Ar–H), 8.12 (d, 8.5 Hz, 1H, Ar–H), 8.10–8.06 (m, 2H, Ar–H), 7.80–7.76 (m, 1H, Ar–H), 7.68–7.64 (m, 1H, Ar–H), 7.41 (d, 8.5 Hz, 1H, Ar–H), 7.07 (d, 2.5 Hz, 1H, Ar–H), 6.94 (dd, 2.5 Hz, 8.5 Hz, 1H, Ar–H), 3.42–3.35 (m, 4H, piperazine–CH_2 × 2), 2.70 (t, 5.0 Hz, 4H, piperazine–CH_2 × 2), 1.40 (s, 9H, CH_3 × 3), 0.86 (s, 9H, CH_3 × 3); ESI-MS: m/z = 699 $[M + H]^+$.

3.1.8. General procedure for the preparation of compounds 16–20. To a solution of intermediate **40** (0.200 mmol) in EA (2.00 mL), EA saturated with hydrogen chloride (2.00 mL) was added dropwise at 0 °C. During this process, a little of the hydrochloride of the Boc-deprotected product precipitated and the suspension was stirred at the room temperature for 3 h. After removal of EA *in vacuo*, the resultant solid was washed with diethylether to give the title compound **16**. Compounds **17–20** were prepared according to the procedure for **16**, only with **40** replaced by **41a–d** as the starting material.

*3.1.8.1. Hydrochloride of N-(4′-((4-(piperazin-1-yl)-3-(trifluoromethyl)phenyl)amino)-[3,6′-biquinolin]-3′-yl)amino (**16**).* Light yellow solid; yield: 94%; ^{1}H NMR (500 MHz, DMSO-d_6): 10.69 (s, 1H, HCl), 9.85 (s, 1H, piperazine–NH), 9.61 (s, 1H, NH), 9.54 (s, 2H, Ar–H), 9.06 (s, 1H, Ar–H), 8.73 (s, 1H, Ar–H), 8.40–8.31 (m, 2H, Ar–H), 8.26 (d, 8.5 Hz, 2H, Ar–H), 8.08–7.98 (m, 1H, Ar–H), 7.93–7.86 (m, 1H, Ar–H), 7.46 (d, 8.5 Hz, 1H, Ar–H), 7.43 (s, 1H, Ar–H), 7.12 (d, 8.5 Hz, 1H, Ar–H), 3.23–3.14 (m, 4H, piperazine–CH_2 × 2), 3.07–2.98 (m, 4H, piperazine–CH_2 × 2); ^{13}C NMR (125 MHz, DMSO-d_6): δ 145.95, 144.81, 141.07, 139.90, 137.90, 134.64, 134.52, 133.86, 133.80, 133.68, 132.83, 132.52, 132.40, 129.78, 129.60, 128.55, 128.10, 126.45 (J_{C-F} 27.50 Hz), 125.22, 124.25 (J_{C-F} 271.25 Hz), 123.61, 123.17, 123.07, 121.78, 117.71 (J_{C-F} 5.00 Hz), 50.39, 43.86; ESI-MS: m/z = 515 $[M + H]^+$; mp 198–200 °C; HPLC: t_R = 12.76 min, flow rate 1.2 mL min^{-1}, COSMOSIL 5C18-MS-II column (4.6 ID × 250 mm), rt, eluent A – 60%, eluent B – 40%.

*3.1.8.2. Hydrochloride of N-(4′-((4-(piperazin-1-yl)-3-(trifluoromethyl)phenyl)amino)-[3,6′-biquinolin]-3′-yl)acetamide (**17**).* Light yellow solid; yield: 97%; ^{1}H NMR (500 MHz, DMSO-d_6): 11.50 (s, 1H, HCl), 9.80 (s, 1H, piperazine–NH), 9.61 (s, 1H, Ar–H), 9.55 (s, 1H, NH), 9.44 (s, 3H, NH, Ar–H × 2), 8.77 (s, 1H, Ar–H), 8.64 (s, 1H, Ar–H), 8.33 (s, 1H, Ar–H), 8.20 (s, 2H, Ar–H), 7.94 (s, 1H, Ar–H), 7.80 (s, 1H, Ar–H), 7.52 (s, 2H, Ar–H), 7.46 (s, 1H, Ar–H), 3.15 (s, 4H, piperazine–CH_2 × 2), 3.08 (s, 4H, piperazine–CH_2 × 2), 1.46 (s, 3H, acetyl); ESI-MS: m/z = 557 $[M + H]^+$; mp 228–230 °C; HPLC: t_R = 10.51 min, flow rate 1.2 mL min^{-1}, COSMOSIL 5C18-MS-II column (4.6 ID × 250 mm), rt, eluent A – 60%, eluent B – 40%.

*3.1.8.3. Hydrochloride of N-(4′-((4-(piperazin-1-yl)-3-(trifluoromethyl)phenyl)amino)-[3,6′-biquinolin]-3′-yl)-methanesulfonamide (**18**).* Light yellow solid; yield: 98%; ^{1}H NMR (500 MHz, DMSO-d_6): 11.21 (s, 1H, HCl), 9.52 (s, 1H, sulfonamide–NH), 9.32 (s, 3H, piperazine–NH, NH, Ar–H), 9.03 (s, 1H, Ar–H), 8.86 (s, 1H, Ar–H), 8.74 (s, 1H, Ar–H), 8.57 (dd, 1.5 Hz, 8.5 Hz, 1H, Ar–H), 8.35 (d, 8.5 Hz, 1H, Ar–H), 8.16 (d, 8.5 Hz, 1H, Ar–H), 8.11 (d, 8.5 Hz, 1H, Ar–H), 7.93–7.87 (m, 1H, Ar–H), 7.80–7.74 (m, 1H, Ar–H), 7.66 (s, 1H, Ar–H), 7.57 (s, 2H, Ar–H), 3.22–3.14 (m, 4H, piperazine–CH_2 × 2), 3.13–3.04 (m, 4H, piperazine–CH_2 × 2), 2.97 (s, 3H, CH_3); ESI-MS: m/z = 593 $[M + H]^+$; mp 245–246 °C; HPLC: t_R = 10.41 min, flow rate 1.2 mL min^{-1}, COSMOSIL 5C18-MS-II column (4.6 ID × 250 mm), rt, eluent A – 60%, eluent B – 40%.

*3.1.8.4. Hydrochloride of 2,2,2-trifluoro-N-(4′-((4-(piperazin-1-yl)-3-(trifluoromethyl)phenyl)amino)-[3,6′-biquinolin]-3′-yl)acetamide (**19**).* Light yellow solid; yield: 93%; ^{1}H NMR (500 MHz, DMSO-d_6): 11.94 (s, 1H, HCl), 11.19 (s, 1H, piperazine–NH), 10.02 (s, 1H, NH), 9.81 (s, 1H, Ar–H), 9.73 (brs, 1H, NH), 9.53 (s, 2H, Ar–H), 8.86 (s, 1H, Ar–H), 8.68 (d, 7.5 Hz, 1H, Ar–H), 8.31 (d, 8.0 Hz, 1H, Ar–H), 8.28 (d, 8.0 Hz, 1H, Ar–H), 8.24 (d, 7.0 Hz, 1H, Ar–H), 8.05–7.99 (m, 1H, Ar–H), 7.91–7.79 (m, 1H, Ar–H), 7.65–7.46 (m, 3H, Ar–H), 3.25–2.99 (m,

7H, piperazine–H), 2.91 (s, 1H, piperazine–H); ^{13}C NMR (125 MHz, DMSO-d_6): δ 155.03 (J_{C-F} 37.50 Hz), 149.99, 148.93, 146.47, 146.66, 146.63, 140.68, 137.56, 136.31, 134.46, 133.75, 132.52, 131.69, 129.69, 129.64, 129.38, 128.54, 126.29 (J_{C-F} 28.75 Hz), 125.09, 124.12, 123.90, 122.84, 123.90 (J_{C-F} 271.25 Hz), 121.95, 121.07, 115.67 (J_{C-F} 287.50 Hz), 112.66, 50.16, 43.79; ESI-MS: m/z = 611 [M + H]$^+$; mp 230–231 °C; HPLC: t_R = 14.78 min, flow rate 1.2 mL min^{-1}, COSMOSIL 5C18-MS-II column (4.6 ID × 250 mm), rt, eluent A – 60%, eluent B – 40%.

3.1.8.5. Hydrochloride of N-(4'-((4-(piperazin-1-yl)-3-(trifluoromethyl)phenyl)amino)-[3,6'-biquinolin]-3'-yl)pivalamide (20). Light yellow solid; yield: 98%; ^{1}H NMR (400 MHz, DMSO-d_6): 11.01 (s, 1H, HCl), 9.67 (s, 1H, piperazine–NH), 9.40 (s, 1H, Ar–H), 9.20–9.10 (m, 4H, Ar–H × 2, NH × 2), 8.79 (s, 1H, Ar–H), 8.62 (d, 8.8 Hz, 1H, Ar–H), 8.33 (d, 8.8 Hz, 1H, Ar–H), 8.14 (d, 8.0 Hz, 2H, Ar–H), 7.90–7.85 (m, 1H, Ar–H), 7.77–7.72 (m, 1H, Ar–H), 7.54 (d, 8.8 Hz, 1H, Ar–H), 7.47 (s, 1H, Ar–H), 7.42 (d, 8.8 Hz, 1H, Ar–H), 3.22–3.15 (m, 4H, piperazine–CH_2 × 2), 3.09–3.02 (m, 4H, piperazine–CH_2 × 2), 0.83 (s, 9H, CH_3 × 3); ESI-MS: m/z = 599 [M + H]$^+$; mp 217–219 °C; HPLC: t_R = 16.66 min, flow rate 1.2 mL min^{-1}, COSMOSIL 5C18-MS-II column (4.6 ID × 250 mm), rt, eluent A – 60%, eluent B – 40%.

3.1.9. General procedure for the preparation of compounds 24–26. To compound **17** (1.0 eq.), anhydrous THF (5 mL per 1 mmol of substrate) and TEA (3.0 eq.) were added. Subsequently, acetyl chloride (1.2 eq.) in anhydrous THF (5 mL per 1 mmol of substrate) was added dropwise to the resultant suspension at 0 °C. The reaction mixture was stirred at the same temperature for 1.5 h and concentrated *in vacuo*. The residue was dissolved in DCM, washed with a saturated $NaHCO_3$ solution and brine. Following removal of DCM *in vacuo*, the residue was subjected to flash column chromatography with EA/MeOH/TEA (50 : 3 : 1) as the eluent to give the target compound **24**.

Compound **25** was prepared according to the procedure for **24**, only with acetyl chloride replaced by methylsulfonyl chloride. Besides, the eluent for flash column chromatography was EA/MeOH/TEA (200 : 4 : 1).

Compound **26** was prepared according to the procedure for **24**, only with **17** replaced by **20** as the starting material. Besides, the eluent for flash column chromatography was EA/MeOH/TEA (200 : 4 : 1).

3.1.9.1. N-(4'-((4-(4-Acetylpiperazin-1-yl)-3-(trifluoromethyl)-phenyl)amino)-[3,6'-biquinolin]-3'-yl)acetamide (24). White solid; yield: 79%; ^{1}H NMR (500 MHz, DMSO-d_6): 9.40 (s, 1H, NH), 9.37 (d, 3.0 Hz, 1H, Ar–H), 9.07 (brs, 1H, NH), 8.77 (s, 2H, Ar–H), 8.64 (d, 2.5 Hz, 1H, Ar–H), 8.26 (dd, 2.5 Hz, 11.0 Hz, 1H, Ar–H), 8.14 (d, 11.0 Hz, 1H, Ar–H), 8.10–8.06 (m, 2H, Ar–H), 7.82–7.77 (m, 1H, Ar–H), 7.70–7.65 (m, 1H, Ar–H), 7.44 (d, 11.0 Hz, 1H, Ar–H), 7.12 (d, 3.0 Hz, 1H, Ar–H), 6.96 (dd, 3.0 Hz, 11.0 Hz, 1H, Ar–H), 3.56–3.51 (m, 4H, piperazine–CH_2 × 2), 2.82–2.78 (m, 2H, piperazine–CH_2), 2.76–2.72 (m, 2H, piperazine–CH_2), 2.03 (s, 3H, acetyl), 1.70 (s, 3H, CH_3, acetyl); ^{13}C NMR (125 MHz, DMSO-d_6): δ 168.75, 168.63, 151.30, 150.10, 147.36, 146.30, 144.54, 140.65, 137.48, 134.71, 133.79, 132.74, 130.59, 130.21, 129.19, 128.88, 128.17, 128.09, 127.63, 126.55 (J_{C-F} 28.75 Hz), 125.46, 124.16, 124.41 (J_{C-F} 271.25 Hz), 122.45, 122.19, 122.03, 115.75 (J_{C-F} 6.25 Hz), 54.06, 53.49, 46.81, 41.92, 23.02, 21.71; ESI-MS: m/z = 599 [M + H]$^+$; mp 195–196 °C; HPLC: t_R = 10.66 min, flow rate 1.2 mL min^{-1}, COSMOSIL 5C18-MS-II column (4.6 ID × 250 mm), rt, eluent A – 70%, eluent B – 30%.

3.1.9.2. N-(4'-((4-(4-(Methylsulfonyl)piperazin-1-yl)-3-(trifluoromethyl)phenyl)amino)-[3,6'-biquinolin]-3'-yl)acetamide (25). Light yellow solid; yield: 84%; ^{1}H NMR (500 MHz, DMSO-d_6): 9.43 (s, 1H, NH), 9.39 (s, 1H, Ar–H), 9.09 (brs, 1H, NH), 8.78 (d, 8.5 Hz, 2H, Ar–H), 8.65 (s, 1H, Ar–H), 8.26 (d, 8.5 Hz, 1H, Ar–H), 8.14 (d, 8.5 Hz, 1H, Ar–H), 8.09 (d, 8.5 Hz, 2H, Ar–H), 7.86–7.76 (m, 1H, Ar–H), 7.73–7.62 (m, 1H, Ar–H), 7.53 (d, 8.5 Hz, 1H, Ar–H), 7.09 (s, 1H, Ar–H), 6.98 (d, 8.5 Hz, 1H, Ar–H), 3.30–3.12 (m, 4H, piperazine–CH_2 × 2), 3.02–2.83 (m, 7H, piperazine–CH_2 × 2, methylsulfonyl), 1.70 (s, 3H, CH_3, acetyl); ESI-MS: m/z = 635 [M + H]$^+$; mp 165–166 °C; HPLC: t_R = 9.18 min, flow rate 1.2 mL min^{-1}, COSMOSIL 5C18-MS-II column (4.6 ID × 250 mm), rt, eluent A – 70%, eluent B – 30%.

3.1.9.3. N-(4'-((4-(4-Acetylpiperazin-1-yl)-3-(trifluoromethyl)-phenyl)amino)-[3,6'-biquinolin]-3'-yl)pivalamide (26). Light yellow solid; yield: 71%; ^{1}H NMR (500 MHz, DMSO-d_6): 9.44 (d, 2.0 Hz, 1H, Ar–H), 9.03 (s, 1H, NH), 8.81 (s, 2H, Ar–H), 8.74 (d, 2.0 Hz, 1H, Ar–H), 8.65 (s, 1H, NH), 8.25 (dd, 2.0 Hz, 8.5 Hz, 1H, Ar–H), 8.12 (d, 8.5 Hz, 1H, Ar–H), 8.10–8.05 (m, 2H, Ar–H), 7.80–7.75 (m, 1H, Ar–H), 7.68–7.64 (m, 1H, Ar–H), 7.40 (d, 8.5 Hz, 1H, Ar–H), 7.08 (d, 2.5 Hz, 1H, Ar–H), 6.95 (dd, 2.5 Hz, 8.5 Hz, 1H, Ar–H), 3.55–3.45 (m, 4H, piperazine–CH_2 × 2), 2.77–2.73 (m, 2H, piperazine–CH_2), 2.71–2.67 (m, 2H, piperazine–CH_2), 2.01 (s, 3H, acetyl), 0.85 (s, 9H, CH_3 × 3); ESI-MS: m/z = 641 [M + H]$^+$; mp 157–159 °C; HPLC: t_R = 16.23 min, flow rate 1.2 mL min^{-1}, COSMOSIL 5C18-MS-II column (4.6 ID × 250 mm), rt, eluent A – 70%, eluent B – 30%.

3.2. mTOR inhibition assay

mTOR inhibitory activity was assessed by Lance ultra assay. mTOR was purchased from Millipore and ATP, DMSO, as well as EDTA, were purchased from Sigma. The kinase buffer contained 50 mM HEPES (pH 7.5), 10 mM $MgCl_2$, 1 mM EDTA, 3 mM MnCl, 0.01% Tween-20 and 2 mM DTT. The kinase solution was prepared by dissolving the kinase in the kinase buffer and the substrate solution was prepared by dissolving the ULight-4E-BP1 peptide substrate and ATP in the kinase reaction buffer. The compound solution, kinase solution and substrate solution were added successively to the wells of the assay plate. The reaction mixture was incubated at room temperature for 1 h, and then stopped by a kinase quench buffer containing EDTA and Eu-anti-phospho-4E-BP1 antibody. Before reading on a plate reader, the mixture needed to be mixed briefly using a centrifuge and was allowed to equilibrate for 60 min. The inhibition rate was

calculated as (max − Lance signal)/(max − min) × 100%. Herein, "max" stands for the DMSO control, while "min" stands for the Lance signal of the no enzyme control. Finally, data were presented in MS Excel and the curves fitted by GraphPad 5.0. The equation used was: Y = Bottom + (Top − Bottom)/(1 + (IC_{50}/X)^HillSlope).

3.3. Cell proliferation assay

Cell proliferation was evaluated by sulforhodamine B (SRB) assay. In detail, HCT116, PC3 and MCF-7 cells were seeded into 96-well plates, cultured overnight and then exposed to serial concentrations of compounds for 72 h. Subsequently, cells were washed with PBS and fixed with 10% (w/v) trichloroacetic acid at 4 °C for 1 h. Afterwards, the cells were stained for 30 min with 0.4% SRB dissolved in 1% acetic acid. Then the cells were washed with 1% acetic acid 5 times, and the protein-bound dye was extracted with 10 mmol of unbuffered Tris base. The absorbance was measured at 515 nm using a multiscan spectrophotometer (Thermo Electron Co., Vantaa, Finland). The inhibition rate on proliferation of each well was calculated as (A515 control cells − A515 treated cells)/A515 control cells ×100%. The average IC_{50} values were determined by the Logit method from at least two independent tests.

3.4. Molecular docking

The co-crystal structure of mTOR in complex with Torin2 (PDB code 4JSX) was used for the docking calculation in C-DOCKER module (Discovery Studio, version 2.5; Accelrys, San Diego, CA, USA, 2008). After removal of Torin2 and solvent molecules, the CHARMm-force field was applied to the protein. The active site was determined according to the location of Torin2 in the mTOR enzyme. After removal of Torin2 from the receptor, each ligand was docked into the defined site. Their final binding conformations were determined based on the calculated CDOCKING ENERGY.

3.5. Class I PI3Ks selectivity assay

PI3Kα inhibitory activity was assessed by Kinase-Glo Luminescent Kinase assay. PI3Kα was purchased from Invitrogen and ATP, DMSO, as well as EDTA, were purchased from Sigma. The kinase buffer contained 50 mM HEPES (pH 7.5), 3 mM $MgCl_2$, 1 mM EDTA, 100 mM NaCl, 0.03% CHAPS and 2 mM DTT. The kinase solution was prepared by dissolving the kinase in the kinase buffer and the substrate solution was prepared by dissolving PIP_2 and ATP in the kinase reaction buffer. The compound solution, kinase solution and substrate solution were added successively to the wells of the assay plate. The reaction mixture was incubated at room temperature for 1 h, and then stopped by the Kinase-Glo reagent. Before reading on a plate reader for luminescence, the mixture needed to be mixed briefly using a centrifuge and was allowed to equilibrate for 15 min. The percent inhibition was calculated as 100 − (max − sample RLU)/(max − min) × 100. Herein, "max" stands for the RLU of the no enzyme control, while "min" means the RLU of the DMSO control. Finally, data were presented in MS Excel and the curves fitted by GraphPad 5.0. The equation used was: Y = Bottom + (Top − Bottom)/(1 + (IC_{50}/X)^HillSlope).

PI3Kβ inhibitory activity was assessed by ADP-Glo Luminescent assay. PI3Kβ was purchased from Millipore and ATP, DMSO, as well as EDTA, were purchased from Sigma. The kinase reaction mixture was incubated at room temperature for 1 h. Afterwards, a little amount of the reaction mixture was transferred to a new 384-well plate and an equal amount of the ADP-Glo reagent was added to each well of the new assay plate to stop the reaction. After being mixed briefly using a centrifuge, the resultant mixture was shaken slowly on the shaker and equilibrated for 40 min. The kinase detection reagent was then added to each well. The mixture was shaken for 1 min, equilibrated for 60 min before reading on a plate reader for luminescence. The percent inhibition was calculated as (max − sample RLU)/(max − min) × 100. Herein, "max" stands for the RLU of the DMSO control, while "min" means the RLU of the no enzyme control. Finally, data were presented in MS Excel and the curves fitted by GraphPad 5.0. The equation used was: Y = Bottom + (Top − Bottom)/(1 + (IC50/X)^HillSlope). PI3Kγ and δ inhibitory activities were evaluated according to the PI3Kβ inhibition assay.

3.6. Western blot analysis

Cells were treated with final concentrations of 0.1 μM or 0.5 μM of **BEZ-235**, rapamycin, compound **24**, and DMSO and incubated at 37 °C for 2 h. Afterwards, the cells were washed twice with ice-cold PBS and cell lysis buffer was added. Then the cellular debris was pelleted by centrifugation at 13 000 rpm for 30 min at 4 °C and the supernatant was collected. For Western blot analysis, the proteins were separated on SDS-PAGE and then transferred onto PVDF membranes. The membranes were incubated with antibodies against pS6 (Ser235) (Cell Signaling Technology), pAkt (Ser473) (Cell Signaling Technology) and GAPDH (Santa Cruz), washed with PBST and then incubated with secondary antibodies. Finally, the proteins were visualized using enhanced chemiluminescence.

3.7. *In vitro* stability assay

The *in vitro* stability in SIF, SGF and RLM was evaluated according to the reported assay with some modification.[27]

4. Conclusions

With the attempt to modify cellular activity of the initial lead **9**, a novel series of 3,4,6-trisubstituted quinoline derivatives were prepared and biologically evaluated *in vitro*. After successive structural optimizations, we discovered several promising quinolines, including **17**, **24** and **25**, which exhibited not only potent mTOR inhibitory activities, but also remarkably enhanced anti-proliferative efficacies compared to **9**. These three quinolines were obtained *via* introducing a ring-

opening strategy to BGT-226, an imidazo[4,5-*c*]quinolinone derivative. Compound **24**, as the most attractive one throughout this series, displayed an IC_{50} value of 30 nM against mTOR, along with IC_{50} values of 0.11, 0.17 and 0.04 μM against the HCT-116, PC-3 and MCF-7 cell lines, respectively. Besides, compounds **17** and **24** were identified to be selective over class I PI3Ks. As illustrated by the further Western blot analysis, compound **24** treatment culminated in a simultaneous inhibition of mTORC1 and mTORC2, thereby beneficial for surmounting the hyper-activation of Akt induced by the S6K/IRS1/PI3K negative feedback loop. Moreover, the representative compound in this series demonstrated acceptable stability in artificial gastric juice, intestinal juice as well as rat liver microsome. Due to these advantages, compounds **17**, **24** and **25** merit further development to investigate their *in vivo* biological profiles.

Acknowledgements

The authors thank Jianyang Pan (Institute of Pharmaceutical Informatics, Zhejiang University, China) for performing NMR spectroscopy and mass spectrometry for structure elucidation.

Notes and references

1 D. D. Sarbassov, S. M. Ali and D. M. Sabatini, *Curr. Opin. Cell Biol.*, 2005, **17**, 596–603.
2 X. M. Ma and J. Blenis, *Nat. Rev. Mol. Cell Biol.*, 2009, **10**, 307–318.
3 D. A. Guertin and D. M. Sabatini, *Cancer Cell*, 2007, **12**, 9–22.
4 G. G. Chiang and R. T. Abraham, *Trends Mol. Med.*, 2007, **13**, 433–442.
5 D. A. Guertin and D. M. Sabatini, *Sci. Signaling*, 2009, **2**, pe24.
6 H. Yang, D. G. Rudge, J. D. Koos, B. Vaidialingam, H. J. Yang and N. P. Pavletich, *Nature*, 2013, **497**, 217–223.
7 D. A. Sabbah, M. G. Brattain and H. Zhong, *Curr. Med. Chem.*, 2011, **18**, 5528–5544.
8 R. J. Shaw and L. C. Cantley, *Nature*, 2006, **441**, 424–430.
9 B. Shor, J. J. Gibbons, R. T. Abraham and K. Yu, *Cell Cycle*, 2009, **8**, 3831–3837.
10 F. Meric-Bernstam and A. M. Gonzalez-Angulo, *J. Clin. Oncol.*, 2009, **27**, 2278–2287.
11 G. Hudes, M. Carducci, P. Tomczak, J. Dutcher, R. Figlin, A. Kapoor, E. Staroslawska, J. Sosman, D. McDermott, I. Bodrogi, Z. Kovacevic, V. Lesovoy, I. G. Schmidt-Wolf, O. Barbarash, E. Gokmen, T. O'Toole, S. Lustgarten, L. Moore and R. J. Motzer, *N. Engl. J. Med.*, 2007, **356**, 2271–2281.
12 R. J. Motzer, B. Escudier, S. Oudard, T. E. Hutson, C. Porta, S. Bracarda, V. Grunwald, J. A. Thompson, R. A. Figlin, N. Hollaender, G. Urbanowitz, W. J. Berg, A. Kay, D. Lebwohl and A. Ravaud, *Lancet*, 2008, **372**, 449–456.
13 C. M. Chresta, B. R. Davies, I. Hickson, T. Harding, S. Cosulich, S. E. Critchlow, J. P. Vincent, R. Ellston, D. Jones, P. Sini, D. James, Z. Howard, P. Dudley, G. Hughes, L. Smith, S. Maguire, M. Hummersone, K. Malagu, K. Menear, R. Jenkins, M. Jacobsen, G. C. Smith, S. Guichard and M. Pass, *Cancer Res.*, 2010, **70**, 288–298.
14 X. Lv, X. Ma and Y. Hu, *Expert Opin. Drug Discovery*, 2013, **8**, 991–1012.
15 S. M. Maira, F. Stauffer, J. Brueggen, P. Furet, C. Schnell, C. Fritsch, S. Brachmann, P. Chene, A. De Pover, K. Schoemaker, D. Fabbro, D. Gabriel, M. Simonen, L. Murphy, P. Finan, W. Sellers and C. Garcia-Echeverria, *Mol. Cancer Ther.*, 2008, **7**, 1851–1863.
16 V. Serra, B. Markman, M. Scaltriti, P. J. Eichhorn, V. Valero, M. Guzman, M. L. Botero, E. Llonch, F. Atzori, S. Di Cosimo, M. Maira, C. Garcia-Echeverria, J. L. Parra, J. Arribas and J. Baselga, *Cancer Res.*, 2008, **68**, 8022–8030.
17 S. D. Knight, N. D. Adams, J. L. Burgess, A. M. Chaudhari, M. G. Darcy, C. A. Donatelli, J. I. Luengo, K. A. Newlander, C. A. Parrish, L. H. Ridgers, M. A. Sarpong, S. J. Schmidt, G. S. Van Aller, J. D. Carson, M. A. Diamond, P. A. Elkins, C. M. Gardiner, E. Garver, S. A. Gilbert, R. R. Gontarek, J. R. Jackson, K. L. Kershner, L. Luo, K. Raha, C. S. Sherk, C. M. Sung, D. Sutton, P. J. Tummino, R. J. Wegrzyn, K. R. Auger and D. Dhanak, *ACS Med. Chem. Lett.*, 2010, **1**, 39–43.
18 B. Markman, F. Atzori, J. Perez-Garcia, J. Tabernero and J. Baselga, *Ann. Oncol.*, 2010, **21**, 683–691.
19 H. M. Cheng, S. Bagrodia, S. Bailey, M. Edwards, J. Hoffman, Q. Y. Hu, R. Kania, D. R. Knighton, M. A. Marx, S. Ninkovic, S. X. Sun and E. Zhang, *MedChemComm*, 2010, **1**, 139–144.
20 A. M. Venkatesan, C. M. Dehnhardt, E. Delos Santos, Z. Chen, O. Dos Santos, S. Ayral-Kaloustian, G. Khafizova, N. Brooijmans, R. Mallon, I. Hollander, L. Feldberg, J. Lucas, K. Yu, J. Gibbons, R. T. Abraham, I. Chaudhary and T. S. Mansour, *J. Med. Chem.*, 2010, **53**, 2636–2645.
21 B. Zheng, J. H. Mao, L. Qian, H. Zhu, D. H. Gu, X. D. Pan, F. Yi and D. M. Ji, *Cancer Lett.*, 2015, **357**, 468–475.
22 Q. Liu, C. Thoreen, J. Wang, D. Sabatini and N. S. Gray, *Drug Discovery Today: Ther. Strategies*, 2009, **6**, 47–55.
23 J. C. Bendell, R. K. Kelley, K. C. Shih, J. A. Grabowsky, E. Bergsland, S. Jones, T. Martin, J. R. Infante, P. S. Mischel, T. Matsutani, S. Xu, L. Wong, Y. Liu, X. Wu, D. S. Mortensen, R. Chopra, K. Hege and P. N. Munster, *Cancer*, 2015, **121**, 3481–3490.
24 D. S. Mortensen, S. M. Perrin-Ninkovic, G. Shevlin, J. Zhao, G. Packard, S. Bahmanyar, M. Correa, J. Elsner, R. Harris, B. G. Lee, P. Papa, J. S. Parnes, J. R. Riggs, J. Sapienza, L. Tehrani, B. Whitefield, J. Apuy, R. R. Bisonette, J. C. Gamez, M. Hickman, G. Khambatta, J. Leisten, S. X. Peng, S. J. Richardson, B. E. Cathers, S. S. Canan, M. F. Moghaddam, H. K. Raymon, P. Worland, R. K. Narla, K. E. Fultz and S. Sankar, *J. Med. Chem.*, 2015, **58**, 5323–5333.
25 K. Y. Chang, S. Y. Tsai, C. M. Wu, C. J. Yen, B. F. Chuang and J. Y. Chang, *Clin. Cancer Res.*, 2011, **17**, 7116–7126.
26 D. P. Qian, A. Q. Han, M. Hamilton and E. Wang, *WO* 2009155527A2, 2009.
27 H. J. Zhou, M. A. Aujay, M. K. Bennett, M. Dajee, S. D. Demo, Y. Fang, M. N. Ho, J. Jiang, C. J. Kirk, G. J. Laidig, E. R. Lewis, Y. Lu, T. Muchamuel, F. Parlati, E. Ring, K. D. Shenk, J. Shields, P. J. Shwonek, T. Stanton, C. M. Sun, C. Sylvain, T. M. Woo and J. Yang, *J. Med. Chem.*, 2009, **52**, 3028–3038.

